COMMUNICATIONS IN COMPUTATIONAL PHYSICS

Large-scale Electromagnetic Modeling for Multiple Inhomogeneous Domains

Masashi Endo, Martin Čuma, and Michael S. Zhdanov*

Department of Geology and Geophysics, University of Utah, 135S 1460E, Rm 719, Salt Lake City, UT 84112, USA

Received 1 May 2008; Accepted (in reviced version) 21 September 2008

Abstract. We develop a new formulation of the integral equation (IE) method for three-dimensional (3D) electromagnetic (EM) field computation in large-scale models with multiple inhomogeneous domains. This problem arises in many practical applications including modeling the EM fields within the complex geoelectrical structures in geophysical exploration. In geophysical applications, it is difficult to describe an earth structure using the horizontally layered background conductivity model, which is required for the efficient implementation of the conventional IE approach. As a result, a large domain of interest with anomalous conductivity distribution needs to be discretized, which complicates the computations. The new method allows us to consider multiple inhomogeneous domains, where the conductivity distribution is different from that of the background, and to use independent discretizations for different domains. This reduces dramatically the computational resources required for large-scale modeling. In addition, using this method, we can analyze the response of each domain separately without an inappropriate use of the superposition principle for the EM field calculations. The method was carefully tested for the modeling the marine controlled-source electromagnetic (MCSEM) fields for complex geoelectric structures with multiple inhomogeneous domains, such as a seafloor with the rough bathymetry, salt domes, and reservoirs. We have also used this technique to investigate the return induction effects from regional geoelectrical structures, e.g., seafloor bathymetry and salt domes, which can distort the EM response from the geophysical exploration target.

AMS subject classifications: 86-08, 86-A25, 86-A60

Key words: large-scale, EM modeling, multiple inhomogeneous domains, marine CSEM.

*Corresponding author. *Email addresses:* masashi.endo@utah.edu (Masashi Endo), mcuma@chpc.utah.edu (Martin Čuma), michael.zhdanov@utah.edu (M. S. Zhdanov)

1 Introduction

The integral equation (IE) method represents an effective computational technique for electromagnetic modeling. In the framework of the IE method, the conductivity distribution is divided into two parts: 1) the background conductivity, σ_b, which is used for the Green's functions calculation, and 2) the anomalous conductivity, $\Delta\sigma_a$, within the domain of integration, D. One principal advantage of the IE method over the other numerical techniques is that the IE method requires discretization of the anomalous domain D only.

It is very well known, however, that the main limitation of the IE method is that the background conductivity model must have a simple structure to allow for an efficient Green's function calculation (Weidelt, 1975; Hohmann, 1975; Wait, 1981; Wannamaker et al., 1984; Xiong, 1992; Pankratov et al., 1995; Zhdanov and Fang, 1997; Zhdanov et al., 2000; Avdeev et al., 2002; Hursán and Zhdanov, 2002). The most widely used background models in EM exploration are those formed by horizontally homogeneous layers. The theory of the Green's functions for layered one-dimensional (1D) models is very well developed and lays the foundation for efficient numerical algorithms. Any deviation from this 1D background model must be treated as an anomalous conductivity.

In many practical geological applications, however, it is difficult to describe an earth structure using the horizontally layered background conductivity model, which is required for the efficient implementation of the conventional IE approach. As a result, a large domain of interest with anomalous conductivity distribution needs to be discretized. This discretization may become too large, however, for a feasible calculation of the fields generated by the geoelectrical structures. Zhdanov et al. (2006) have recently developed a method to address this problem, the inhomogeneous background conductivity (IBC) IE method This method is based on the separation of the effects due to excess electric current, $\mathbf{j}^{\Delta\sigma_b}$, induced in the inhomogeneous background domain, from those due to the anomalous electric current, $\mathbf{j}^{\Delta\sigma_a}$, in the location of the anomalous conductivity. As a result, we arrive at a system of integral equations which uses the same simple Green's functions for the layered model as in the original IE formulation. In order to take into account the return induction effects of the anomalous domain to the inhomogeneous background domain, the IBC IE method can be applied iteratively (Zhdanov et al., 2006; Endo et al., 2007).

We have extended this iterative IBC IE method to the modeling of multiple inhomogeneous domains. In the framework of this method, we can construct a model with any number of inhomogeneous domains and take into account the return induction effects between any pairs of the inhomogeneous domains by using the iterative method. The important point is that by using this method we can evaluate the individual response from every domain, which includes the possible EM coupling effects between the different domains. A rigorous separate calculation of the EM fields produced by different anomalous domains representing different geological structures (e.g., a salt dome and a hydrocarbon (HC) reservoir) represents an important practical problem of EM exploration. Indeed. In the marine CSEM method, an inhomogeneous structure, such as the seafloor with the rough bathymetry or a salt dome, can distort the response of an HC reservoir, which is the main target of the survey.

In summary, in this paper we not only demonstrate the effectiveness of the new forward modeling method but also examine the effects of the EM coupling between the different inhomogeneous domains which can distort a useful EM anomaly and complicate the interpretation of the marine CSEM data.

2 Integral equation formulation for multiple inhomogeneous domain modeling

In this section we summarize the principles of the IE method of EM modeling with multiple inhomogeneous domains. We assume that N inhomogeneous domains (D_i, $i=1,\ldots,N$) are located within a horizontally layered earth (Figure 1). The conductivity of the horizontally layered earth (normal conductivity) is σ_n, while the inhomogeneous (anomalous) conductivity within each inhomogeneous domain is denoted as $\Delta\sigma_{D_i}$ ($i=1,\ldots,N$). The total EM fields at any point $\mathbf{r}$, $\mathbf{E}^t(\mathbf{r})$, and $\mathbf{H}^t(\mathbf{r})$, can be expressed as a sum of normal fields $\mathbf{E}^n(\mathbf{r})$, $\mathbf{H}^n(\mathbf{r})$, and the EM fields induced by every inhomogeneous domain $\mathbf{E}^{\Delta\sigma_{D_i}}(\mathbf{r})$, $\mathbf{H}^{\Delta\sigma_{D_i}}(\mathbf{r})$ ($i=1,\ldots,N$):

$$\mathbf{E}^t(\mathbf{r}) = \mathbf{E}^n(\mathbf{r}) + \sum_{i=1}^{N} \mathbf{E}^{\Delta\sigma_{D_i}}(\mathbf{r}) = \mathbf{E}^n(\mathbf{r}) + \sum_{i=1}^{N} G_E^{D_i}\left[\Delta\sigma_{D_i}\mathbf{E}^t\right], \tag{2.1}$$

$$\mathbf{H}^t(\mathbf{r}) = \mathbf{H}^n(\mathbf{r}) + \sum_{i=1}^{N} \mathbf{H}^{\Delta\sigma_{D_i}}(\mathbf{r}) = \mathbf{H}^n(\mathbf{r}) + \sum_{i=1}^{N} G_H^{D_i}\left[\Delta\sigma_{D_i}\mathbf{E}^t\right], \tag{2.2}$$

where $G_E^{D_i}$ and $G_H^{D_i}$ are electric and magnetic Green's operators acting within domain D_i, respectively. Then the EM modeling problem is reduced to the calculation of the total electric fields inside each inhomogeneous domain.

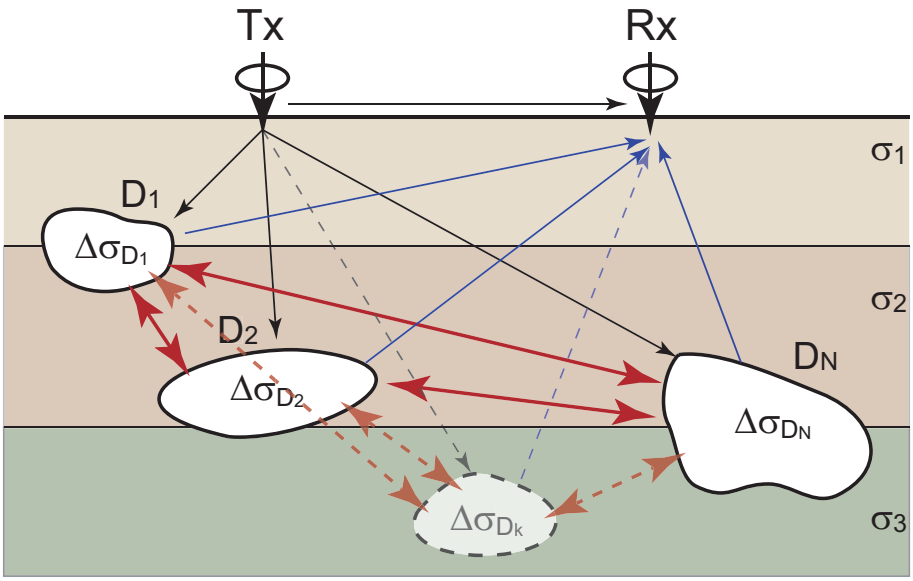

Figure 1: A sketch of a 3D geoelectrical model with horizontally layered (normal) conductivity and N inhomogeneous conductivities.

Rearranging the equation (2.1) for the electric field induced in inhomogeneous domain D_N, we have:

$$\mathbf{E}^{\Delta\sigma_{D_N}}(\mathbf{r}) = \mathbf{E}^t(\mathbf{r}) - \mathbf{E}^n(\mathbf{r}) - \sum_{i=1}^{N-1} \mathbf{E}^{\Delta\sigma_{D_i}}(\mathbf{r}). \tag{2.3}$$

In practice, at the first step of the field calculation, we do not know the values of any electric fields in equation (2.3). We thus first calculate the electric field in domain D_1 without taking into account the induction effect from any other domains:

$$\mathbf{E}^{\Delta\sigma_{D_1}}(\mathbf{r}) = G_E^{D_1}\left[\Delta\sigma_{D_1}\mathbf{E}^t\right] = \mathbf{E}^t(\mathbf{r}) - \mathbf{E}^n(\mathbf{r}). \tag{2.4}$$

Equation (2.4) can be written as an integral equation with respect to the field $\mathbf{E}^{\Delta\sigma_{D_1}}$:

$$\mathbf{E}^{\Delta\sigma_{D_1}}(\mathbf{r}) = G_E^{D_1}\left[\Delta\sigma_{D_1}\left(\mathbf{E}^n + \mathbf{E}^{\Delta\sigma_{D_1}}\right)\right]. \tag{2.5}$$

This integral equation is solved using the contraction form of integral equations (Hursán and Zhdanov, 2002) and the complex generalized minimal residual (CGMRES) method (Zhdanov, 2002).

In the calculation of the field due to the currents induced in the next domain (2), we take into account the electric field induced from the inhomogeneous domain 1, $\mathbf{E}^{\Delta\sigma_{D_1}}(\mathbf{r})$:

$$\mathbf{E}^{\Delta\sigma_{D_2}}(\mathbf{r}) = G_E^{D_2}\left[\Delta\sigma_{D_2}\mathbf{E}^t\right] = \mathbf{E}^t(\mathbf{r}) - \mathbf{E}^n(\mathbf{r}) - \mathbf{E}^{\Delta\sigma_{D_1}}(\mathbf{r}). \tag{2.6}$$

The last equation is equivalent to the following integral equation:

$$\mathbf{E}^{\Delta\sigma_{D_2}}(\mathbf{r}) = G_E^{D_2}\left[\Delta\sigma_{D_2}\left(\mathbf{E}^n + \mathbf{E}^{\Delta\sigma_{D_2}} + \mathbf{E}^{\Delta\sigma_{D_1}}\right)\right], \tag{2.7}$$

which is solved again by the CGMRES method.

Finally, for the last inhomogeneous domain D_N, we already know the electric fields in all the other inhomogeneous domains and thus we can calculate the electric field $\mathbf{E}^{\Delta\sigma_{D_N}}(\mathbf{r})$ as described by equation (2.3).

To improve the accuracy, we can use this scheme iteratively. In the subsequent iterations, we use the fields obtained in the previous iteration to calculate the induced fields in the given domain. For example, in the second iteration, the calculation of the electric fields from the inhomogeneous domain D_1 will use the electric fields from other domains obtained in the first iteration as:

$$\mathbf{E}_{(2)}^{\Delta\sigma_{D_1}}(\mathbf{r}) = \mathbf{E}_{(1)}^t(\mathbf{r}) - \mathbf{E}^n(\mathbf{r}) - \sum_{i=2}^{N} \mathbf{E}_{(1)}^{\Delta\sigma_{D_i}}(\mathbf{r}), \tag{2.8}$$

where the numerical field subscripts denote the iteration number. The electric fields from the other inhomogeneous domains are calculated similarly, always using the latest obtained electric fields for the given domain. For example, for the electric fields due to the domain (2) at the second iteration:

$$\mathbf{E}_{(2)}^{\Delta\sigma_{D_2}}(\mathbf{r}) = \mathbf{E}_{(1)}^t(\mathbf{r}) - \mathbf{E}^n(\mathbf{r}) - \sum_{i=3}^{N} \mathbf{E}_{(1)}^{\Delta\sigma_{D_i}}(\mathbf{r}) - \mathbf{E}_{(2)}^{\Delta\sigma_{D_1}}(\mathbf{r}). \tag{2.9}$$

This process is repeated until the electric fields within all the inhomogeneous domains reach self consistency, i.e., the norm of difference between the electric fields in any domain at iterations i and $(i-1)$ is less than a certain threshold ε. In the kth inhomogeneous domain, for example, the electric fields satisfy the following inequality:

$$\frac{\left\| \mathbf{E}_{(i)}^{\Delta\sigma_{D_k}}\left(\mathbf{r}_j\right) - \mathbf{E}_{(i-1)}^{\Delta\sigma_{D_k}}\left(\mathbf{r}_j\right) \right\|_2}{\left\| \mathbf{E}_{(i)}^{\Delta\sigma_{D_k}}\left(\mathbf{r}_j\right) \right\|_2} < \varepsilon, \quad \mathbf{r}_j \in D_k. \tag{2.10}$$

The developed multiple-domain integral equation (MD IE) method is implemented in a new version of the parallel computer code PIE3D_MD. We will present the results of numerical modeling using this new algorithm and code in the following sections.

3 Validity of the MD IE method

The new parallel computer code PIE3D MD can model the low-frequency EM field propagation within the conductive medium for a set of several types of transmitters, which include: (1) plane wave, (2) horizontal/vertical electric bipoles (with the finite length), (3) rectangular/circular loops, (4) magnetic dipoles in all three (x, y, and z) directions. In order to check the accuracy of a new method/code, we have applied the MD IE method (PIE3D_MD) to a simple numerical model to analyze its efficiency in comparison with the conventional IE modeling, obtained by PIE3D code, which has been already published (Yoshioka and Zhdanov, 2005) and it is widely used by EM geophysical community. This method and the corresponding computer code was extensively cross-checked and validated by multiple comparisons with the analytical solutions and the results obtained by FD and FE methods.

Figure 2 shows a sketch of Model 1 selected for this modeling experiment. In the case of calculations using MD IE method, we consider three separate anomalous domains representing three resistive rectangular prisms, domains 1, 2, and 3, embedded in a two-layered half-space. In the case of the conventional IE method we consider one anomalous domain covering all three bodies as shown in Figure 2. The resistivities of the inhomogeneous domains are 30, 30, and 100 ohm-m and that of the background are 0.3 and 1 ohm-m. The thickness of the first layer is 1350 m.

The EM field in this model is excited by an x-directed electric horizontal bipole with a length of 270 m, which is located at the points with horizontal coordinates from 0 to 20 km (every 200 m) in the x direction. The elevation of the transmitter bipole is 50 m above the layer boundary. The transmitter generates the frequency-domain EM field at a frequency of 0.25 Hz. The electric field receiver is located at $x = 7500$ m on x axis, as shown in Figure 2.

Following the main principles of the MD IE method for multiple inhomogeneous domains, the modeling area is divided into three modeling domains, D_1, D_2, and D_3. We use 960 ($12 \times 8 \times 10$) cells with a cell size of $250 \times 250 \times 100$ m^3 for discretizations of D_1 and D_2, while D_3 is discretized into 256 ($16 \times 8 \times 2$) cells with a cell size of $250 \times 250 \times 100$ m^3. For the case of calculation by conventional IE method, the anomalous domain D_a is discretized into 4160 ($52 \times 8 \times 10$) cells with a cell size of $250 \times 250 \times 100$ m^3.

Figure 3 shows the convergence plots for the calculation of the EM field for Model 1. It took just four iterations of the MD IE method to converge to the given level of the threshold $\varepsilon = 10^{-4}$.

Figure 4 shows the amplitude-versus-offset (AVO) plots of the x (in-line) component of the anomalous electric fields (left-hand panel), and z (vertical) compoent (right-hand panel). The solid lines represent the results obtained by the conventional IE method (PIE3D), whereas the circles represent those computed using a new MD IE method (PIE3D_MD). One can see that both results agree well with each other.

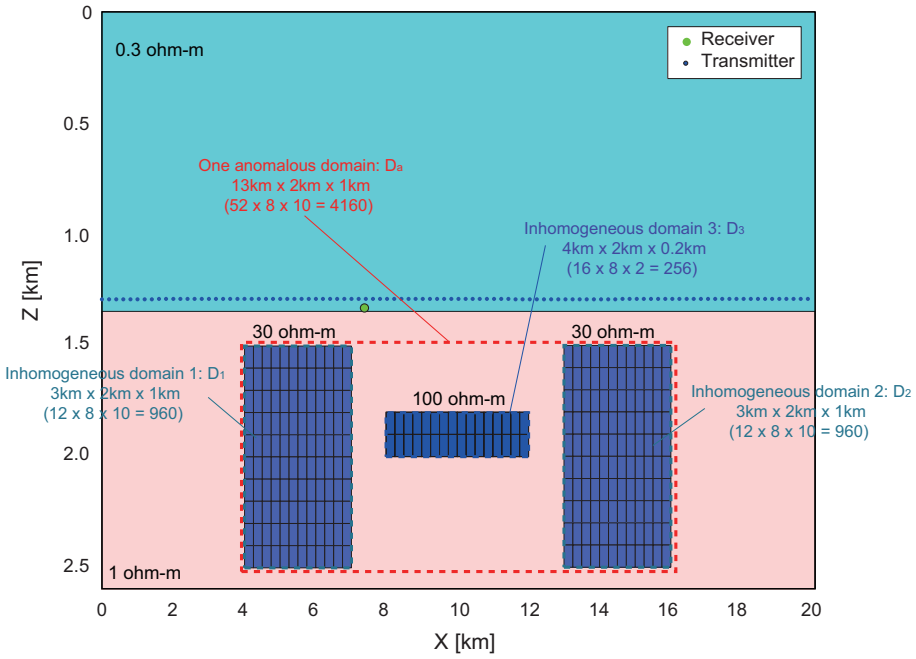

Figure 2: A sketch of Model 1 used to test the validity of the MD IE method.

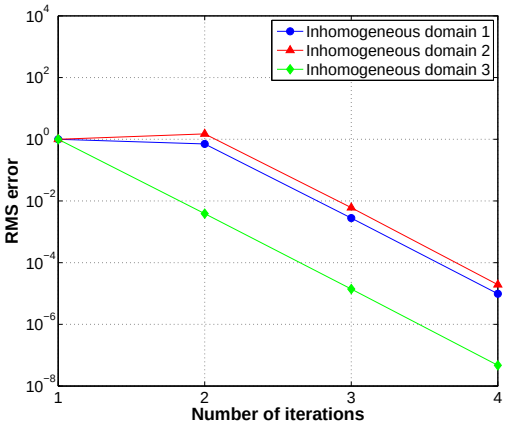

Figure 3: Convergence plots for the calculation of the EM field for Model 1.

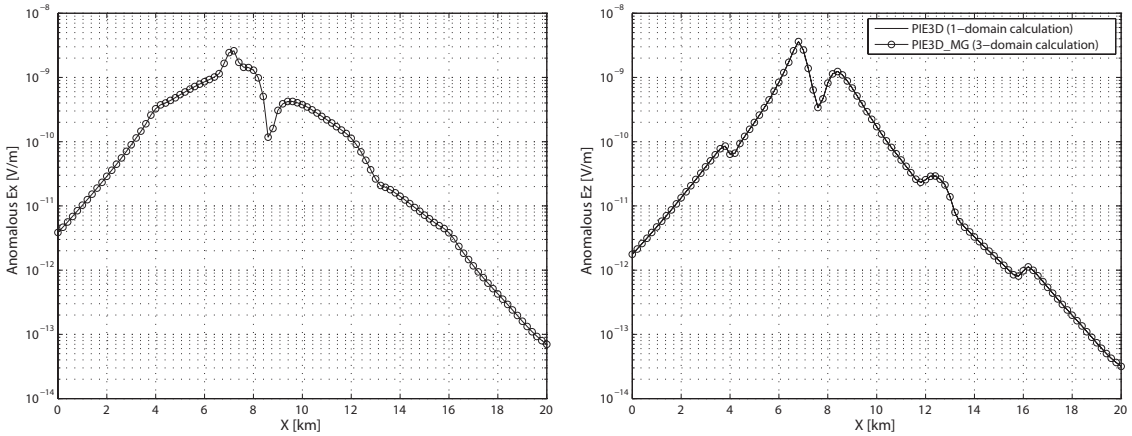

Figure 4: The amplitude-versus-offset (AVO) plots of the x (in-line) component of the anomalous electric fields (left-hand panel), and z (vertical) compoent (right-hand panel). The solid lines show the results by conventional IE method (PIE3D), while the circles indicate the results by MD IE method (PIE3D_MD).

Figure 5 shows the phase-versus-offset (PVO) plots of the x (in-line) component of the anomalous electric fields (left-hand panel), and z (vertical) compoent (right-hand panel). As same as the case of the AVO plots, one can see that both results agree well with each other.

4 Application of the MD IE method for studying the EM coupling effects in marine CSEM data

In this section we will present the application of the developed MD IE method and a new version of the PIE3D_MD code for computer simulation of the EM coupling effects in marine CSEM data collected over the areas with a rough sea bottom bathymetry. This is a very important problem in marine EM geophysics, because the effect of the sea bottom bathymetry can significantly distort the useful EM response from a hydrocarbon (HC) reservoir, which is the main target of offshore geophysical exploration. As a prototype of the seafloor bathymetry structure in all our models we use the known seafloor bathymetry of the Sabah area, Malaysia. Sarawak Shell Berhad, Shell International Exploration and Production, and PETRONAS Managing Unit have conducted an MCSEM study to test the viability of the technology by acquiring data over geologically favorable target reservoirs in the Sabah area in 2004. They also carried out a survey for the seafloor bathymetry. We have used a simplified model of the seafloor bathymetry data provided by Shell in constructing the geoelectrical models considered in this paper. A 3D relief of the true seafloor bathymetry of Sabah area, Malaysia, is plotted in Figure 6.

4.1 Three-domain model (seafloor bathymetry, plus a salt dome, plus an HC reservoir, Model 2)

A vertical section of the geoelectrical structure of Model 2 is shown in Figure 7. This figure shows a resistive HC reservoir with a resistivity of 100 ohm-m and a salt dome with a resistivity of

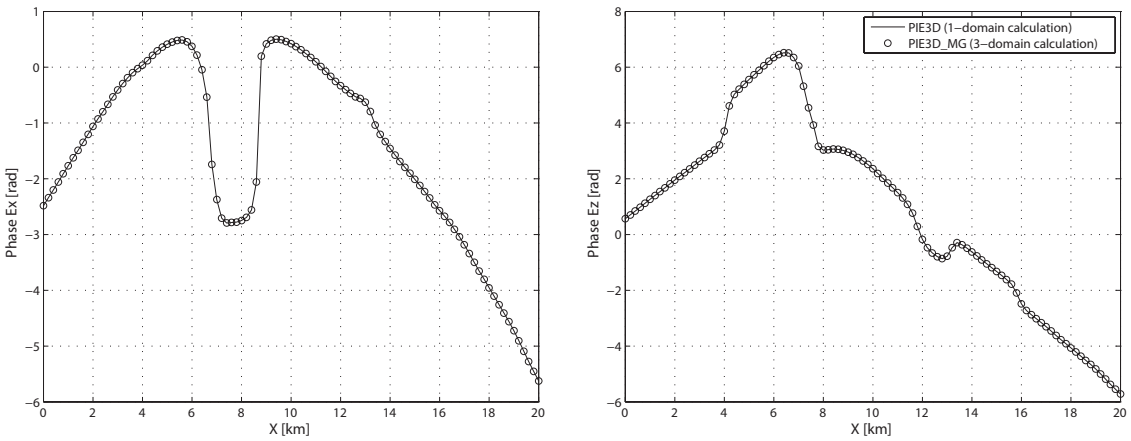

Figure 5: The phase-versus-offset (PVO) plots of the x (in-line) component of the anomalous electric fields (left-hand panel), and z (vertical) compoent (right-hand panel). The solid lines show the results by conventional IE method (PIE3D), while the circles indicate the results by MD IE method (PIE3D_MD).

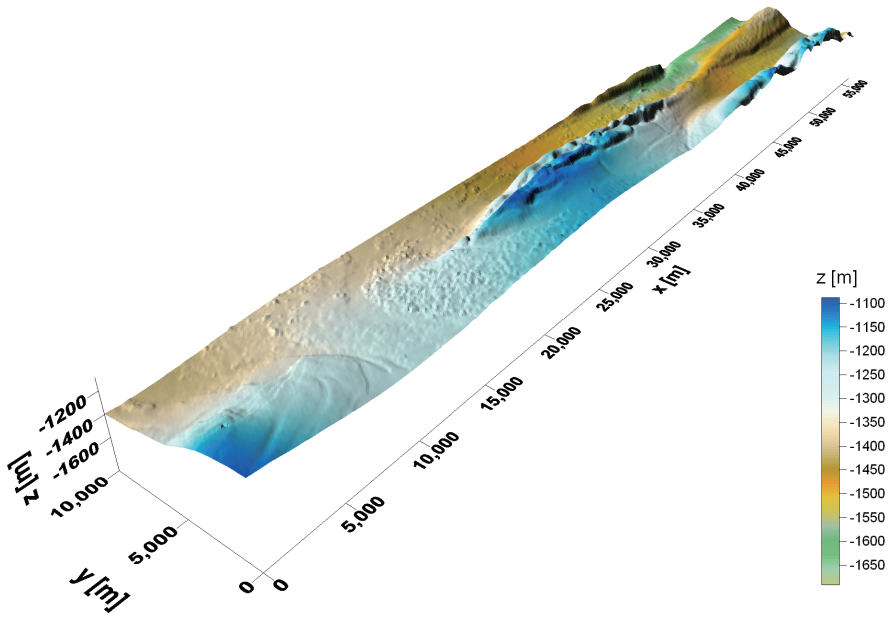

Figure 6: A 3D relief of the seafloor bathymetry for the Sabah model.

30 ohm-m located within conductive sea-bottom sediments whose resistivity is 1 ohm-m. The resistivity of the seawater layer is 0.3 ohm-m, and the depth of the seafloor is from 1200 m to 1350 m below sea level.

The EM field in this model is excited by an x-directed electric horizontal bipole with a length of 270 m, which is located at the points with horizontal coordinates from 0 to 20 km (every 200 m) in the x direction and from -3 km to 3 km (every 200 m) in the y direction. The elevation of the transmitter bipole is 50 m above the sea bottom. The transmitter generates the frequency-domain EM field at a frequency of 0.25 Hz. The electric field receivers are located along the y axis at the points with horizontal coordinates from 5.5 km to 13.5 km (1-km spacing; 8 points), as shown in Figure 7.

The modeling area is divided into three modeling domains, D_1, D_2, and D_3, outlined by the dashed lines in Figure 7. Modeling domain D_1 covers the area with conductivity variations associated with the bathymetry of the sea bottom, while modeling domains D_2 and D_3 correspond to the location of the salt dome and the HC reservoir, respectively. We use 120,000 ($200 \times 60 \times 10$) cells with a cell size of $100 \times 100 \times 25$ m^3 for a discretization of the seafloor bathymetry structure. Domain D_2 of the salt dome area is discretized into 36960 ($35 \times 24 \times 44$) cells with a cell size of $100 \times 100 \times 25$ m^3, and domain D_2 of the reservoir area is discretized into 12800 ($40 \times 40 \times 8$) cells with a cell size of $100 \times 100 \times 25$ m^3.

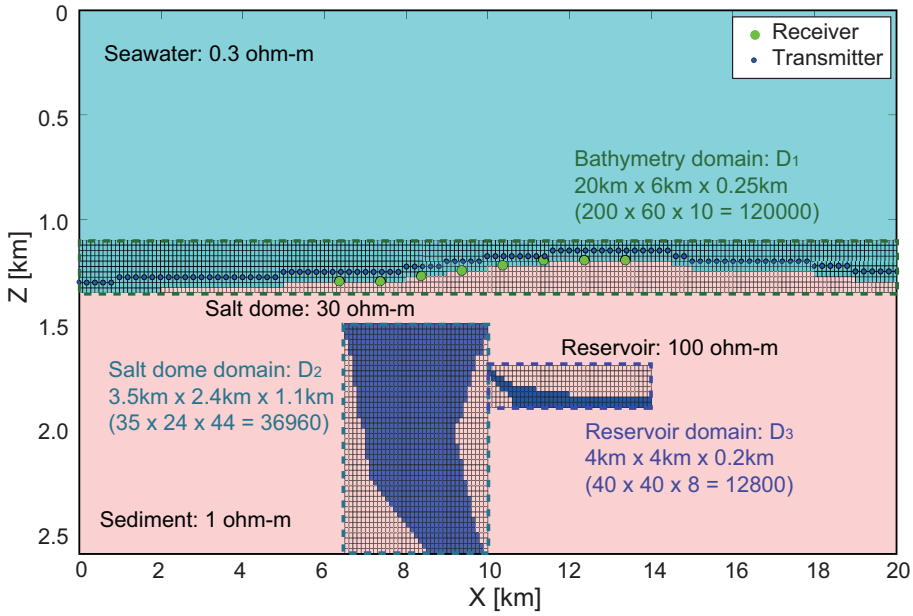

Figure 7: A vertical geoelectrical section of Model 2.

We use four CPUs (Opteron 2.0 GHz) for this calculation. The calculation time is around 43 min, and the required memory and the disc space are around 1.0 GB and 7.3 GB, respectively. It took just seven iterations of the MD IE method to converge to the given level of the threshold $\varepsilon = 10^{-4}$ (Figure 8).

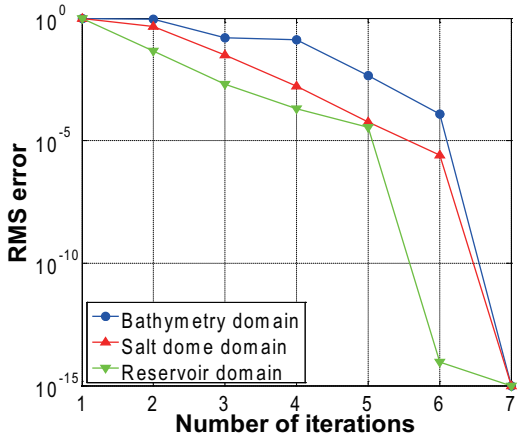

Figure 8: Convergence plots for the calculation of the EM field for Model 1.

4.1.1 Analysis of the maps of the amplitude of the electric fields observed at sea bottom

Figures 9 and 10 present maps of the absolute values of the x (in-line) and z (vertical) components of the total electric field calculated by the MD IE method at the sea bottom for transmitter # 1 ($x = 5.5$ km). The gray cross indicates the position of the transmitter, and the white and the dark blue dashed lines represent the horizontal locations of the salt dome and of the reservoir, respectively. One can see that the total electric fields become larger in the area close to the receiver and distorted slightly by the presence of the inhomogeneous domains (salt dome and reservoir).

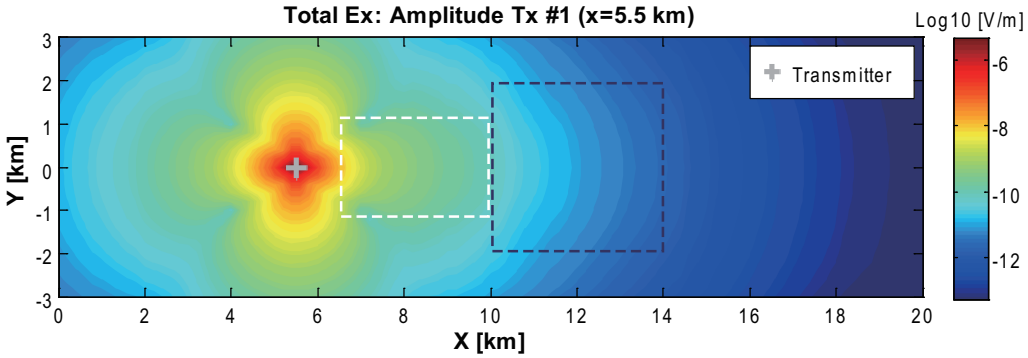

Figure 9: Model 2: A map of the absolute values of the x (in-line) component of the total electric field at sea bottom, for transmitter # 1 ($x = 5.5$ km).

Figures 11 and 12 show maps of the absolute values of the x (in-line) and z (vertical) components of the anomalous electric field generated by the currents induced in the reservoir domain only, calculated by the MD IE method, which includes the return induction effects from all the other domains (seafloor bathymetry and salt dome). It is clear from these figures that both of the

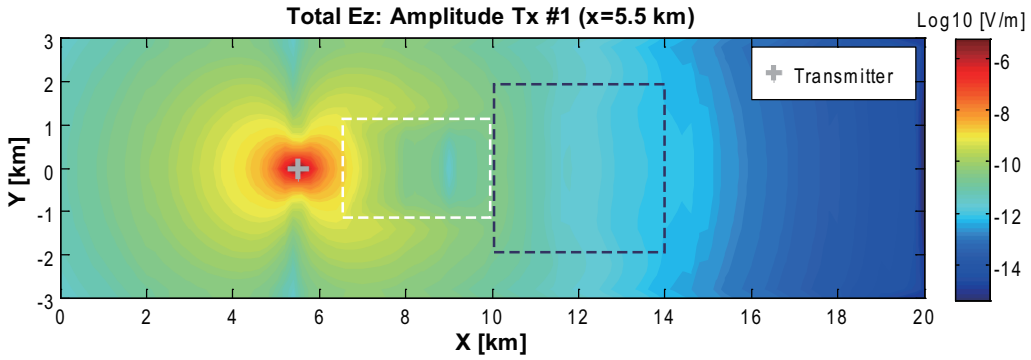

Figure 10: Model 2: A map of the absolute values of the z (vertical) component of the total electric field at sea bottom for transmitter $\#$ 1 ($x=5.5$ km).

components of the anomalous field associated with the reservoir are concentrated in the horizontal location of the reservoir.

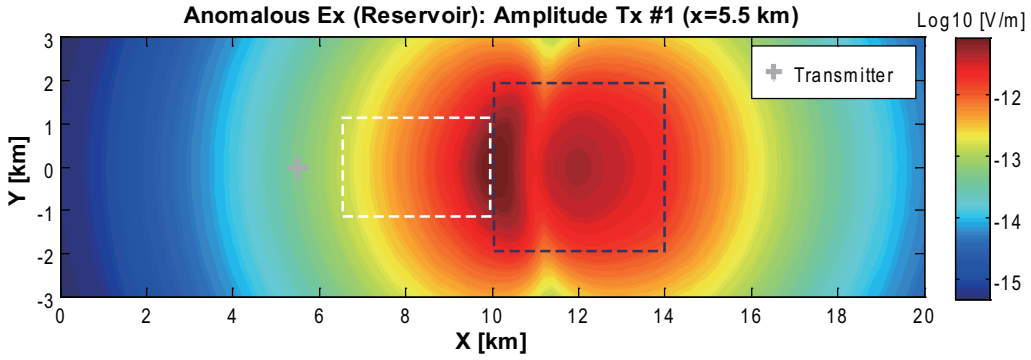

Figure 11: Model 2: A map of the absolute values of the x (in-line) component of the anomalous electric field generated by the currents induced in the reservoir domain only.

Figures 13 and 14 show maps of the absolute values of the x (in-line) and z (vertical) components of the anomalous electric field generated by the currents induced in the salt dome domain only, calculated by the MD IE method. As in the case of the response from the reservoir, both of the components of the anomalous fields are concentrated in the horizontal location of the salt dome.

4.1.2 Analysis of the amplitude-versus-offset (AVO) plots of the electric fields

Figures 15 and 16 show the amplitude-versus-offset (AVO) plots of the electric fields calculated by the MD IE method for the x (in-line) and z (vertical) components, respectively. One can see that, due to the EM coupling between the different inhomogeneous domains, the normalized AVO plots become very complicated. In this situation it is difficult to evaluate the horizontal location of the reservoir (or a salt dome) from these plots.

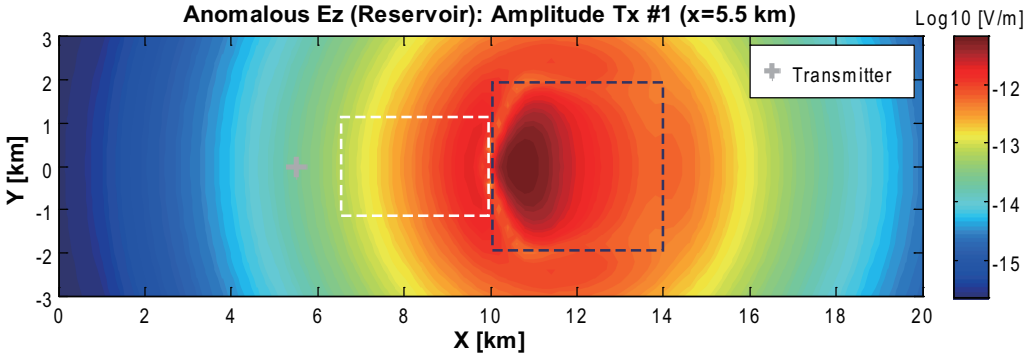

Figure 12: Model 2: A map of the absolute values of the z (vertical) component of the anomalous electric field generated by the currents induced in the reservoir domain only.

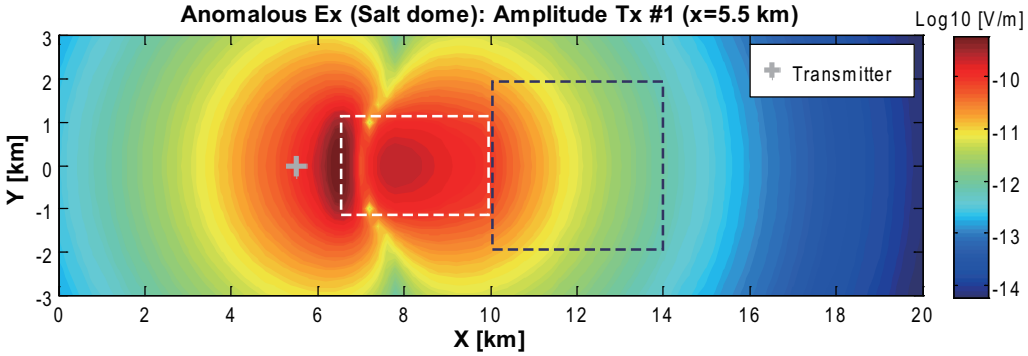

Figure 13: Model 2: A map of the absolute values of the x (in-line) component of the anomalous electric field generated by the currents induced in the salt dome domain only.

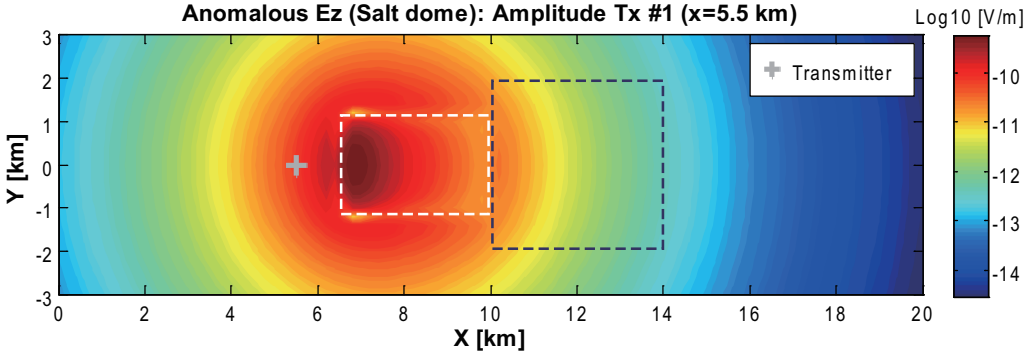

Figure 14: Model 2: A map of the absolute values of the z (vertical) component of the anomalous electric field generated by the currents induced in the salt dome domain only.

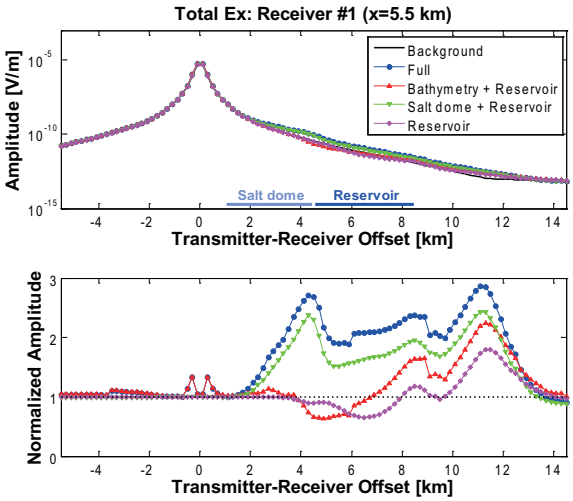

Figure 15: The top panel shows amplitude-versus-offset (AVO) plots of the x (in-line) component of the electric fields at receiver $\#1$ ($x = 5.5$ km). The bottom panel presents the AVO plots of the same fields normalized by the absolute values of the normal electric fields. We use the following codes for the curves: 1) "Background" corresponds to the normal field in the horizontally layered background model; 2) "Full" corresponds to the total field in the model; 3) "Bathymetry + Reservoir" corresponds to the sum of the normal field and the anomalous fields due to the seafloor bathymetry and reservoir domains; 4) "Salt dome + Reservoir" corresponds to the sum of the normal field and the anomalous fields due to the salt dome and reservoir domains; 5) "Reservoir" corresponds to the sum of the normal field and the anomalous field due to the reservoir domain only.

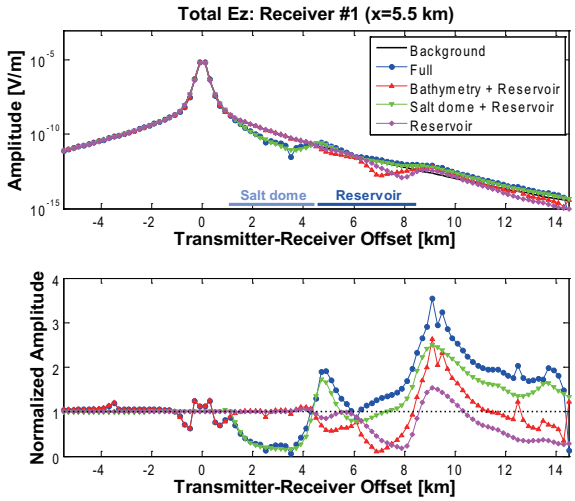

Figure 16: The top panel shows amplitude-versus-offset (AVO) plots of the z (vertical) component of the electric fields at receiver $\#1$ ($x = 5.5$ km). The bottom panel presents the AVO plots of the same fields normalized by the absolute values of the normal electric fields. We use the following codes for the curves: 1) "Background" corresponds to the normal field in the horizontally layered background model; 2) "Full" corresponds to the total field in the model; 3) "Bathymetry + Reservoir" corresponds to the sum of the normal field and the anomalous fields due to the seafloor bathymetry and reservoir domains; 4) "Salt dome + Reservoir" corresponds to the sum of the normal field and the anomalous fields due to the salt dome and reservoir domains; 5) "Reservoir" corresponds to the sum of the normal field and the anomalous field due to the reservoir domain only.

4.1.3 Comparison of the anomalous fields from the HC reservoir domain in different geoelectrical models

We have already indicated that the conventional amplitude-versus-offset (AVO) plots do not provide clear information about the horizontal location of the target in the complex case of a geoelectrical model formed by several inhomogeneous domains representing a seafloor bathymetry, a salt dome, and a reservoir. This is caused by the EM coupling effect between the different domains. Figures 17 and 18 represent the amplitude versus offset (AVO) plots of the x (in-line) and z (vertical) components of the anomalous field due to the reservoir domain only. These plots were computed using three different models: 1) a full model, containing seafloor bathymetry, salt dome, and reservoir domains; 2) a "bathymetry + reservoir" model, without a salt dome structure; 3) a "salt dome + reservoir" model, without a seafloor bathymetry structure. "Reservoir model calculations" were made for the model containing the reservoir domain only. For example, the anomalous field computed for the "reservoir model calculation" does not include any return induction effects from a salt dome and/or seafloor bathymetry because we calculate this field in the model which contains a reservoir domain only.

We can see that the response of the reservoir (anomalous field) changes if the model includes other inhomogeneous domains, i.e., if the return induction effects are present in the model. The same changes can occur in the fields due to the other domains. Therefore, the behavior of the total field, which is computed by taking into account the coupling between the different domains with anomalous conductivity, can be very different from a field obtained by a simple superposition of the individual anomalous fields due to the individual domains. This property of the observed EM field reflects the nonlinearity of the EM induction problem. In other words, a simple superposition principle, which is widely used in potential (e.g., gravity) field theory cannot be applied in modeling EM data.

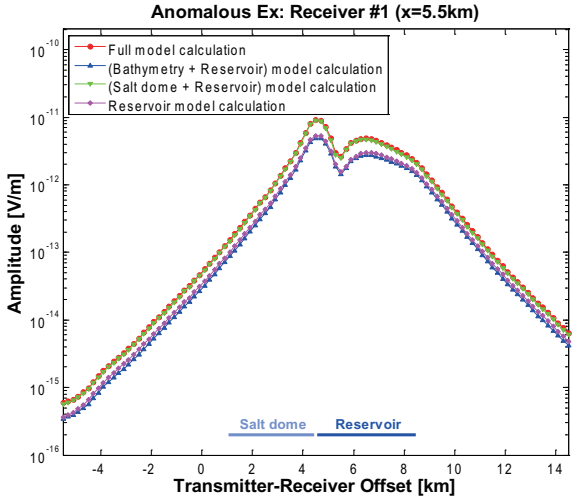

Figure 17: Amplitude-versus-offset (AVO) plots of the x (in-line) component of the anomalous field due to the reservoir domain only. These plots were computed using four different models: 1) "Full model calculation" including seafloor bathymetry, salt dome, and reservoir domains; 2) "Bathymetry + reservoir" model, without a salt dome structure; 3) "Salt dome + reservoir" model, without a seafloor bathymetry structure; 4) "Reservoir model calculations" for the model containing a reservoir domain only.

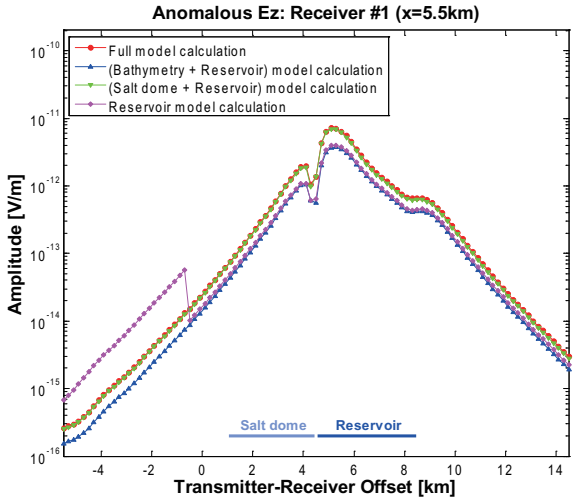

Figure 18: Amplitude-versus-offset (AVO) plots of the z (vertical) component of the anomalous field due to the reservoir domain only. These plots were computed using four different models: 1) "Full model calculation" including seafloor bathymetry, salt dome, and reservoir domains; 2) "Bathymetry + reservoir" model, without a salt dome structure; 3) "Salt dome + reservoir" model, without a seafloor bathymetry structure; 4) "Reservoir model calculations" for the model containing a reservoir domain only.

4.1.4 Comparison of the normalized AVO plots

Next, we have investigated the normalized AVO plots. Usually the amplitude of the EM field is normalized by the normal (layered background) field. Because we can calculate the response from the EM currents induced in each domain by our MD IE method, we can use any combination of these fields (not only the normal field) to normalize the AVO plots. Figures 19 and 20 show the AVO plots of the total electric fields (calculated for the full geoelectrical model containing seafloor bathymetry, salt dome, and reservoir domains) normalized by normal (layered background), "normal + bathymetry," "normal + salt dome," and "full" (normal + seafloor bathymetry + salt dome) fields.

These figures demonstrate that we can evaluate the horizontal location of the reservoir more easily by using the total field normalized by the field which is calculated as a sum of the currents induced in all domains except for the target domain (in this case, except for the field of the reservoir domain). In the practical data we observed the total field, which includes the EM coupling effects from all the inhomogeneities. Therefore, in the numerical modeling one should calculate the response of all the known inhomogeneous domains in order to be able to detect the location of the target effectively.

4.2 Four-domain model (seafloor bathymetry, plus two salt domes, plus a reservoir, Model 3)

We have calculated an EM field for a model which includes four domains (a seafloor bathymetry, two salt domes, and a reservoir) to investigate the code performance for a model with many domains, and to study the multiple domain effect in the data. A vertical section of the geoelectrical

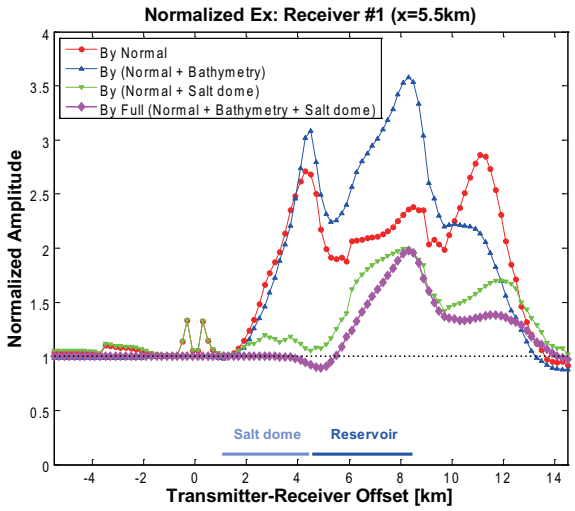

Figure 19: AVO plots of the total in-line electric field (calculated for a full geoelectrical model containing seafloor bathymetry, salt dome, and reservoir domains) normalized by normal (layered background), "normal + bathymetry," "normal + salt dome," and "full" (normal + seafloor bathymetry + salt dome) fields.

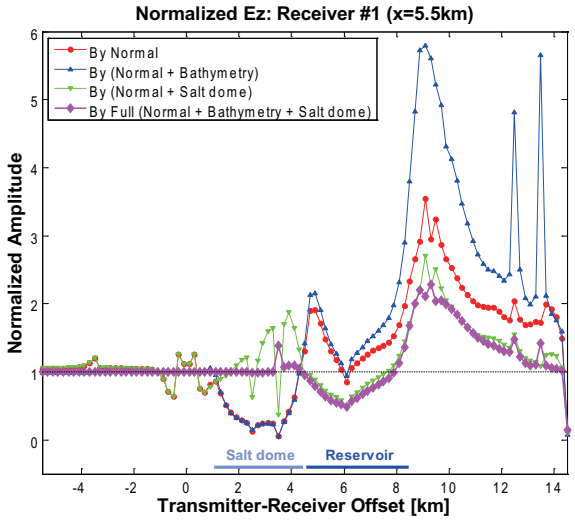

Figure 20: AVO plots of the total vertical component of the electric field (calculated for a full geoelectrical model containing seafloor bathymetry, salt dome, and reservoir domains) normalized by normal (layered background), "normal + bathymetry," "normal + salt dome," and "full" (normal + seafloor bathymetry + salt dome) fields.

structure of Model 3 is shown in Figure 21. One can see in this figure that the geoelectrical model is formed by a resistive HC reservoir with a resistivity of 100 ohm-m, two salt domes with a resistivity of 30 ohm-m are located within the conductive sea-bottom sediments whose resistivity is 1 ohm-m. The resistivity of the seawater layer is 0.3 ohm-m, and the depth of the seafloor is from 1200 m to 1350 m below sea level.

The EM field in this model is excited by an x-directed electric horizontal bipole with a length of 270 m and located at the points with horizontal coordinates from 0 to 20 km (every 200 m) in the x direction and from -3 to 3 km (every 200 m) in the y direction. The elevation of the transmitter bipole is 50 m above the sea bottom. The transmitter generates the frequency-domain EM field at a frequency of 0.25 Hz. The electric field receivers are located along the y axis at the points with horizontal coordinates from 7.5 to 13.5 km (2-km spacing), as shown in Figure 21.

Following the main principles of the MD IE method for multiple inhomogeneous domains, the modeling area was represented by four modeling domains, D_1, D_2, D_3 and D_4, outlined by the dashed lines in Figure 21. Modeling domain D_1 covers the area with conductivity variations associated with the bathymetry of the sea bottom, while modeling domains D_2 and D_3 correspond to the location of the salt domes. Modeling domain D_4 corresponds to the location of the HC reservoir. We used 20160 (80 $\times$ 24 $\times$10) cells with a cell size of 250 $\times$ 250 $\times$25 m^3 for a discretization of the seafloor bathymetry structure. Each of the domains D_2 and D_3 of the salt dome areas was discretized into 1280 (16 $\times$ 8 $\times$10) cells with a cell size of 250 $\times$ 250 $\times$100 m^3, and the domain D_4 of the reservoir area was discretized into 2000 (25 $\times$ 20 $\times$4) cells with a cell size of 200 $\times$ 200 $\times$25 m^3.

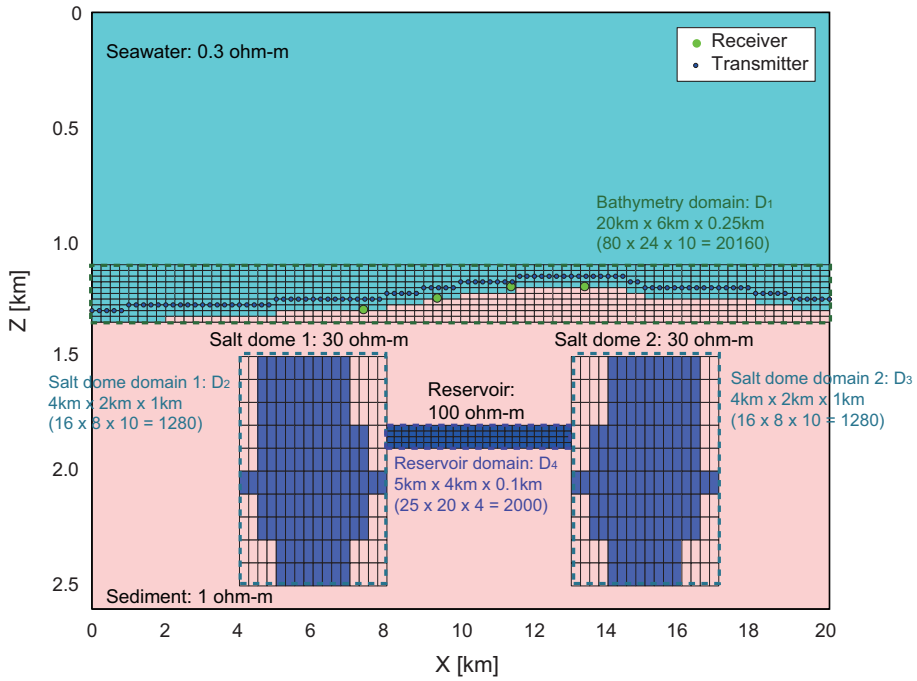

Figure 21: A vertical section of the geoelectrical structure of Model 3.

We use four CPUs (Opteron 2.0 GHz) for this calculation. The calculation time is around 12

min, and the required memory and the disc space are around 100 MB and 750 MB, respectively. It took just seven iterations of the MD IE method to converge to the given level of the threshold $\varepsilon = 10^{-4}$ (Figure 22).

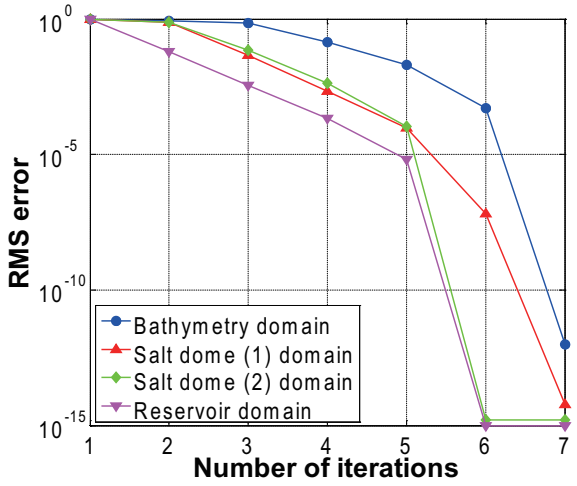

Figure 22: Convergence plots for the calculation of the EM field for Model 3.

Figures 23 and 24 present maps of the absolute values of the x (in-line) and z (vertical) components of the total electric field calculated by the MD IE method at the sea bottom for transmitter # 2 ($x = 9.5$ km). The gray cross indicates the position of the transmitter, and the white and the dark blue dashed lines represent the horizontal locations of the salt domes and the reservoir, respectively.

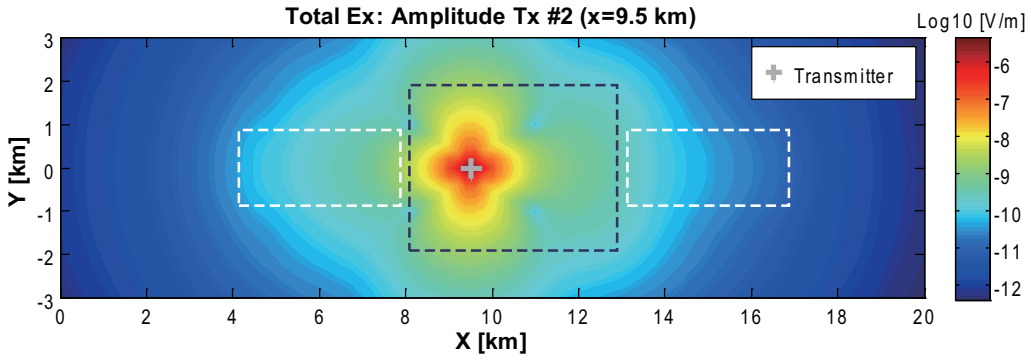

Figure 23: Model 3: A map of the absolute values of the x (in-line) component of the total electric field at sea bottom, for transmitter #2 ($x = 9.5$ km).

Figures 25 and 26 show maps of the absolute values of the x (in-line) and z (vertical) components of the anomalous electric field generated by the currents induced in the reservoir domain only, calculated by the MD IE method, which includes the return induction effects from all the

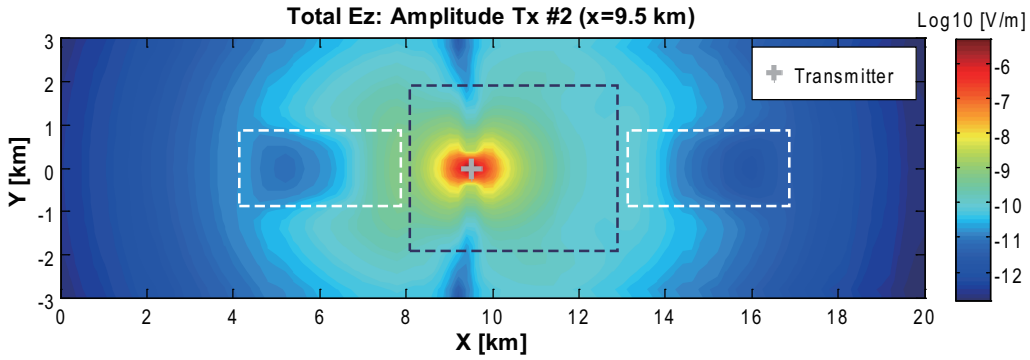

Figure 24: Model 3: A map of the absolute values of the z (vertical) component of the total electric field at sea bottom, for transmitter $\#2$ ($x = 9.5$ km).

other domains (seafloor bathymetry and salt domes). It is clear from these figures that both of the components of the anomalous field associated with the reservoir are concentrated in the horizontal location of the reservoir.

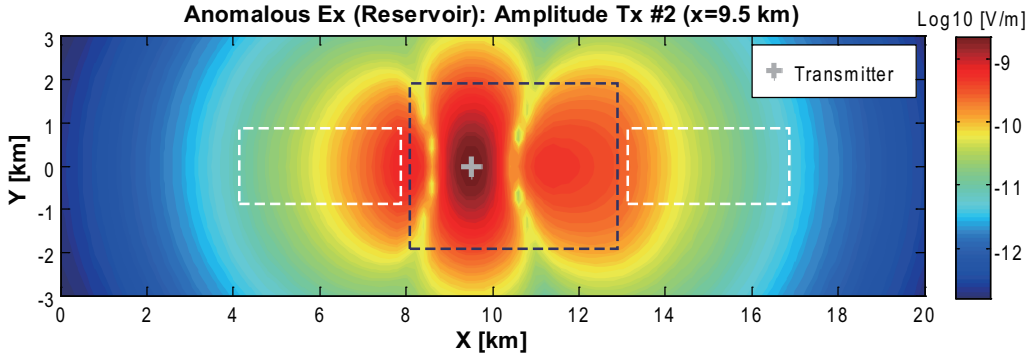

Figure 25: Model 3: A map of the absolute values of the x (in-line) component of the anomalous electric field generated by the currents induced in the reservoir domain only.

Figures 27 and 28 show maps of the absolute values of the x (in-line) and z (vertical) components of the anomalous electric field generated by the currents induced in the salt dome domains only, calculated by the MD IE method. One can see that the anomalous field is concentrated in the horizontal location of the salt dome now.

4.3 Five-domain model (seafloor bathymetry, plus two salt domes, plus two reservoirs, Model 4)

In the final numerical experiment, we have calculated an EM field for a model which includes five domains. A vertical section of Model 4 is shown in Figure 29. We just added an extra reservoir domain, D_5, to Model 3. All other parameters of the model are the same as those for Model 3.

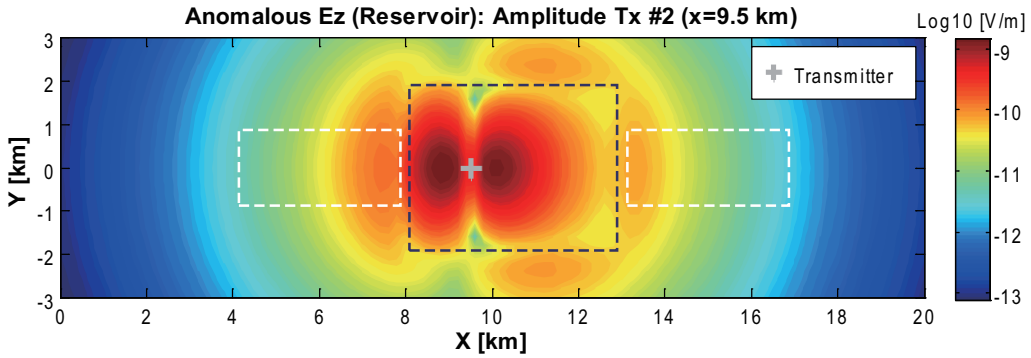

Figure 26: Model 3: A map of the absolute values of the z (vertical) component of the anomalous electric field generated by the currents induced in the reservoir domain only.

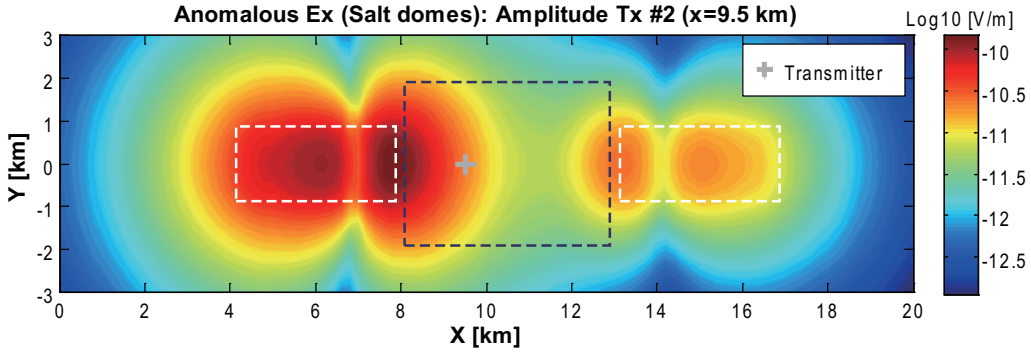

Figure 27: Model 3: A map of the absolute values of the x (in-line) component of the anomalous electric field generated by the currents induced in the salt dome domains only.

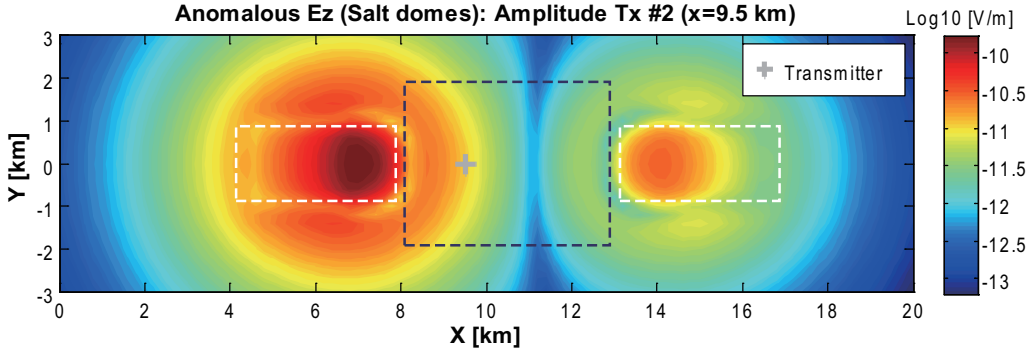

Figure 28: Model 3: A map of the absolute values of the z (vertical) component of the anomalous electric field generated by the currents induced in the salt dome domains only.

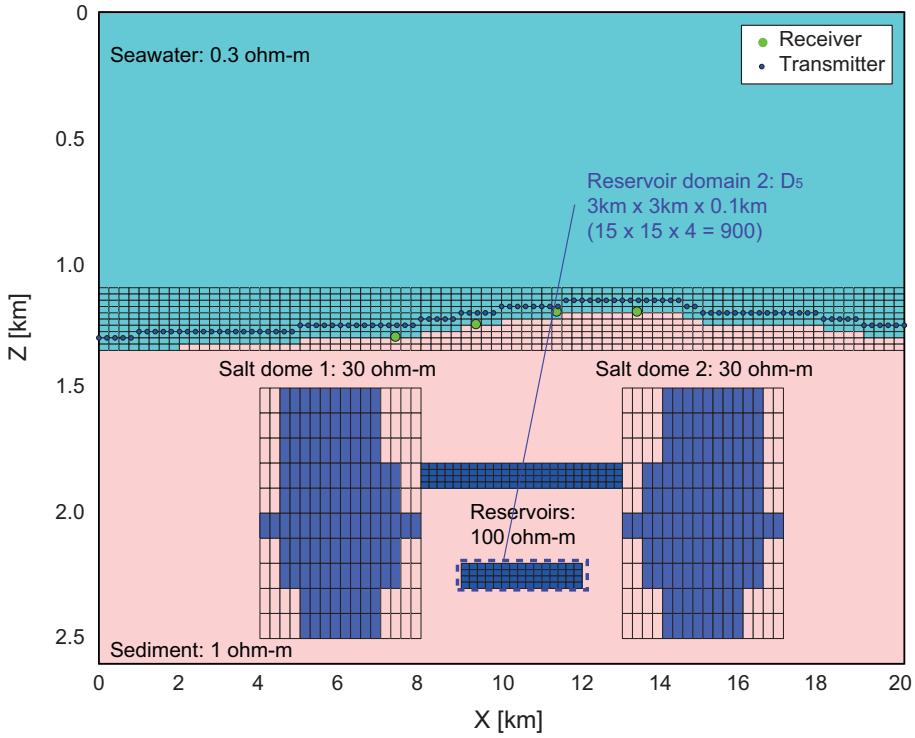

Figure 29: A vertical geoelectrical section of Model 4.

We use four CPUs (Opteron 2.0 GHz) for this calculation. The calculation time is around 23 min, and the required memory and the disc space are around 100 MB and 1 GB, respectively. It took ten iterations of the MD IE method to converge to the given level of the threshold $\varepsilon = 10^{-4}$ (Figure 30).

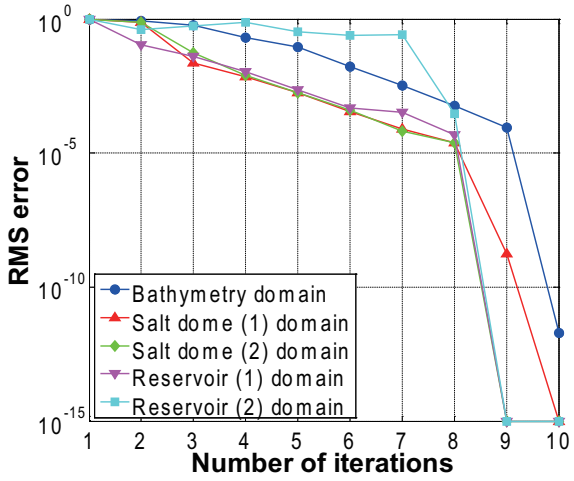

Figure 30: Convergence plots for the calculation of the EM field for Model 4.

Figures 31 and 32 present maps of the absolute values of the x (in-line) and z (vertical) components of the total electric field calculated by the MD IE method at the sea bottom for transmitter # 2 ($x = 9.5$ km). The gray cross indicates the position of the transmitter, and the white and the dark blue dashed lines represent the horizontal locations of the salt domes and the reservoirs, respectively.

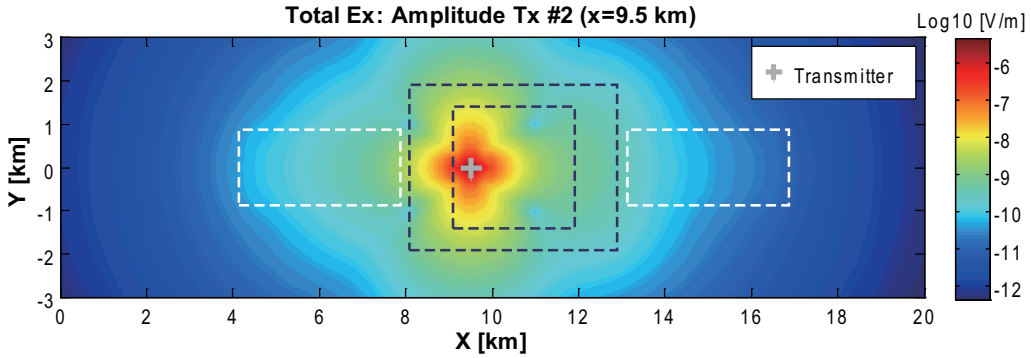

Figure 31: Model 4: A map of the absolute values of the x (in-line) component of the total electric field at sea bottom, for transmitter #2 ($x = 9.5$ km).

Figures 33 and 34 show maps of the absolute values of the x (in-line) and z (vertical) components of the anomalous electric field generated by the currents induced in the reservoir domains only, calculated by the MD IE method, which includes the return induction effects from all other

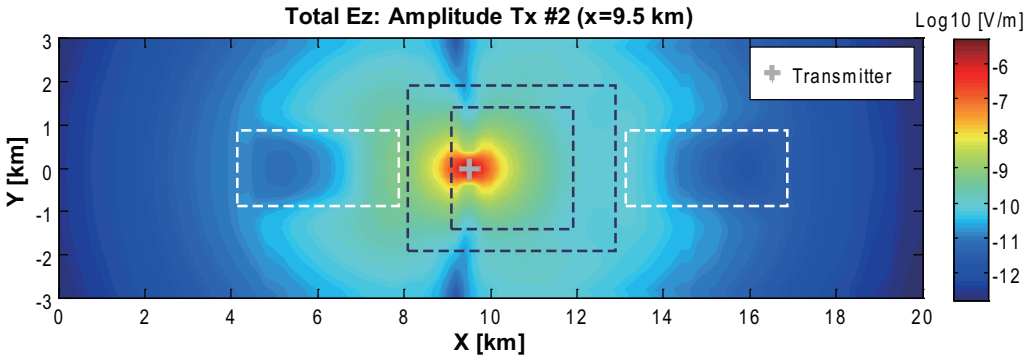

Figure 32: Model 4: A map of the absolute values of the z (vertical) component of the total electric field at sea bottom, for transmitter $\#2$ ($x=9.5$ km).

domains (seafloor bathymetry and salt dome).We can see that the anomalous field associated with the reservoirs is concentrated in the horizontal location of the reservoirs.

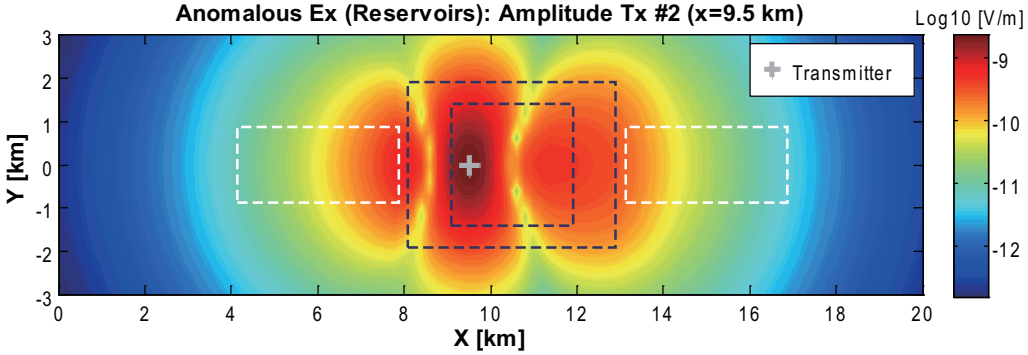

Figure 33: Model 4: A map of the absolute values of the x (in-line) component of the anomalous electric field generated by the currents induced in the reservoir domains only.

Figures 35 and 36 show maps of the absolute values of the x (in-line) and z (vertical) components of the anomalous electric field generated by the currents induced in the salt dome domains only, calculated by the MD IE method. In this case, the anomalous fields are concentrated in the horizontal location of the salt domes.

5 Conclusions

In this paper we introduce a new MD IE method which can be used for the complex geoelectrical models with multiple inhomogeneous domains. This method is based on the extension of the original IBC IE method. Contrary to the finite-difference (FD), or finite element (FE) techniques, the new MD IE method requires discretization of the domains with the anomalous conductivity only.

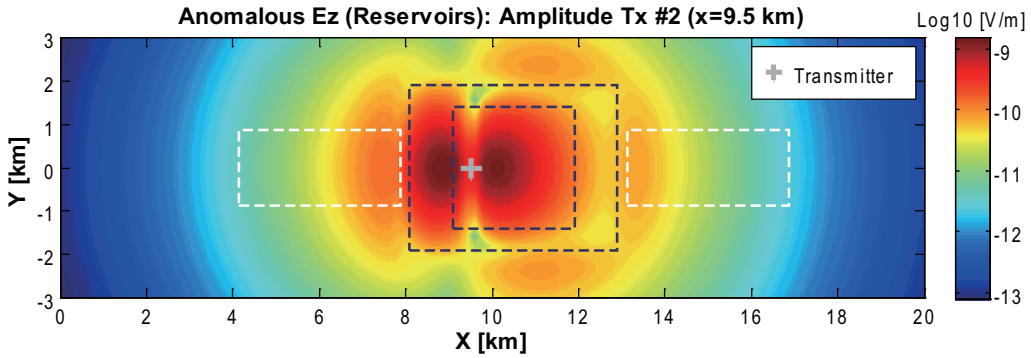

Figure 34: Model 4: A map of the absolute values of the z (vertical) component of the anomalous electric field generated by the currents induced in the reservoir domains only.

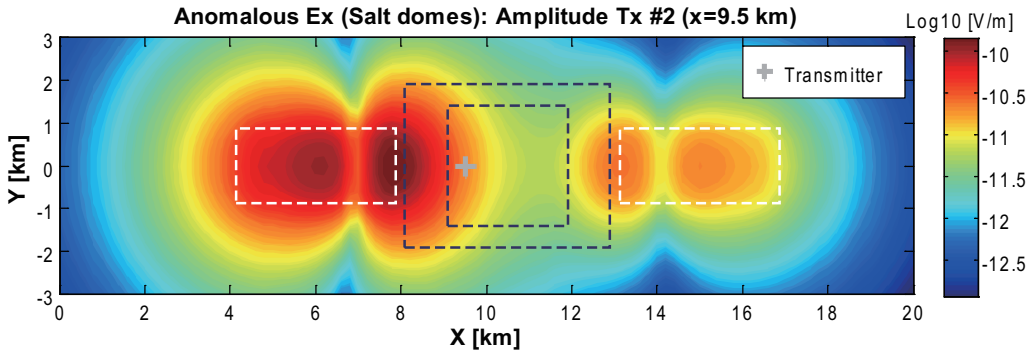

Figure 35: Model 4: A map of the absolute values of the x (in-line) component of the anomalous electric field generated by the currents induced in the salt dome domains only.

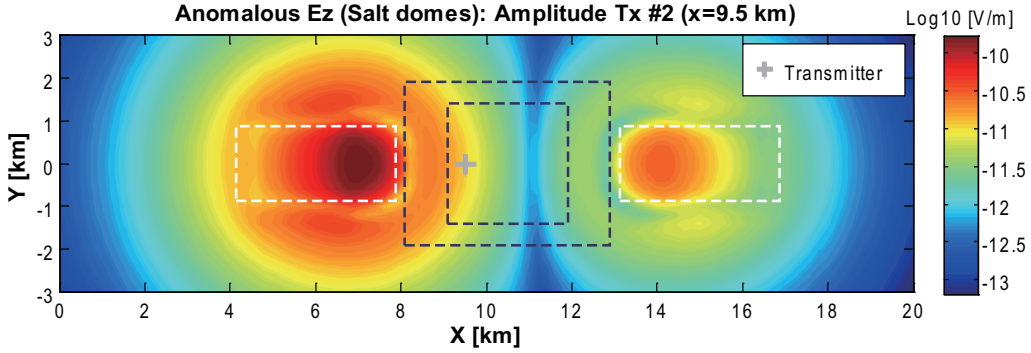

Figure 36: Model 4: A map of the absolute values of the z (vertical) component of the anomalous electric field generated by the currents induced in the salt dome domains only.

Also, in the majority of the conventional IE methods, the FFT method is used for the fast integration over the inhomogeneous domain. In this case, even if we have two anomalous bodies located far apart from each other, we have to define one "anomalous domain," which would include both bodies in the calculations by the conventional IE method. Contrary to this situation, the new developed MD IE method can treat these two anomalous bodies as two different inhomogeneous domains, so that we do not have to discretize the large region covering both domains.

At the same time, the new method provides a rigorous solution of the EM modeling problem by taking into account the EM coupling between the different domains. In addition, because the MD IE approach is based on the IE method, we can analyze the response of each domain separately, without an inappropriate use of the superposition principle for the EM field calculations.

Using the new modeling facility, we have examined the MCSEM data for the models with multiple inhomogeneous domains, including seafloor bathymetry, salt dome, and reservoir structures. The numerical modeling results demonstrate that the new modeling method can be effectively used for studying the EM fields in complex geoelectrical models with multiple inhomogeneous domains.

Acknowledgments

The authors are thankful to Dr. Mark Rosenquist of Shell for providing the Sabah area seafloor bathymetry data and permission to publish the modeling results.

We also acknowledge the support of the University of Utah Consortium for Electromagnetic Modeling and Inversion (CEMI), which includes BAE Systems, Baker Atlas Logging Services, BGP China National Petroleum Corporation, BHP Billiton World Exploration Inc., BP, Centre for Integrated Petroleum Research, EMGS, ENI S.p.A., ExxonMobil Upstream Research Company, FUGRO, Halliburton, INCO Exploration, Information Systems Laboratories, MTEM, Newmont Mining Co., Norsk Hydro, OHM, Petrobras, Rio Tinto - Kennecott, Rocksource, Russian Research Center Kurchatov Institute, Schlumberger, Science Applications International Co., Shell International Exploration and Production Inc., Statoil, Sumitomo Metal Mining Co., and Zonge Engineering and Research Organization.

References

[1] Avdeev, D. B., A. V. Kuvshinov, O. V. Pankratov, and G. A. Newman, 2002, Three dimensional induction logging problems, part I, An integral equation solution and model comparison: Geophysics, **67**, 413–426.

[2] Endo, M., M. Čuma, and M. S. Zhdanov, 2007, Multigrid IE method for large-scale model with inhomogeneous backgrounds: 77th Annual International Meeting, SEG, Expanded Abstract.

[3] Hohmann, G. W., 1975, Three-dimensional induced polarization and EM modeling: Geophysics, **40**, 309–324.

[4] Hursán, G., and M. S. Zhdanov, 2002, Contraction integral equation method in three-dimensional electromagnetic modeling: Radio Science, **37**, 1089–2002.

[5] Pankratov, O. V., D. B. Avdeev, and A. V. Kuvshinov, 1995, Scattering of electromagnetic field in inhomogeneous earth: Forward problem solution, Izv. Akad. Nauk SSSR Fiz. Zemli, **3**, 17–25.

[6] Wait, J. R., 1981, Wave propagation theory: Pergamon Press.

[7] Wannamaker, P. E., G. W. Hohmann, and W. A. SanFilipo, 1984, Electromagnetic modeling of three dimensional bodies in layered earths using integral equations: Geophysics, **49**, 60–74.
[8] Weidelt, P., 1975, EM induction in three-dimensional structures: J. Geophysics, **41**, 85–109.
[9] Xiong, Z., 1989, Electromagnetic fields of electrical dipoles embedded in a stratified anisotropic earth: Geophysics, **54**, 1643–1646.
[10] Yoshioka, K., and M. S. Zhdanov, 2005, Electromagnetic forward modeling based on the integral equation method using parallel computers: 75th Annual International Meeting, SEG, Expanded Abstracts.
[11] Zhdanov, M. S., and S. Fang, 1997, Quasi-linear series in three-dimensional electromagnetic modeling: Radio Sci., **32**, 2167–2188.
[12] Zhdanov, M. S., V. I. Dmitriev, S. Fang, and G. Hursán, 2000, Quasi-analytical approximations and series in electromagnetic modeling: Geophysics, **65**, 1746–1757.
[13] Zhdanov, M.S., 2002, Geophysical inverse theory and regularization problems: Elsevier.
[14] Zhdanov, M. S., S. K. Lee, and K. Yoshioka, 2006, Integral equation method for 3D modeling of electromagnetic fields in complex structures with inhomogeneous background conductivity: Geophysics, **71**, G333–G345.